Transport through a one–dimensional quantum dot

T. Kleimann[a], M. Sassetti[a], G. Cuniberti[b], and B. Kramer[c]

[a]Dipartimento di Fisica, INFM, Università di Genova,
Via Dodecaneso 33, I–16146 Genova, Italy
[b]Max-Planck-Institut für Physik komplexer Systeme,
Nöthnitzer Straße 38, D–01187 Dresden, Germany
[c] I. Institut für Theoretische Physik, Universität Hamburg,
Jungiusstraße 9, D–20355 Hamburg, Germany

Abstract

We examine the effects of long-range interactions in a quantum wire with two impurities. We employ the bosonization technique and derive an effective action for the system. The effect of the long-range interaction on the charging energy and spectral properties of the island formed by the impurities and the linear transport is discussed.

1 Introduction

Considerable progress in the fabrication of quasi one-dimensional nanostructures has been made in recent years. Such quantum wires are ideal tools for studying the interplay of impurities and interaction effects. It is even possible to form one–dimensional quantum dots [1] and investigate their transport properties in the linear and nonlinear regime where the latter gives insight into the spectral properties of the system. In quantum wires fabricated by the cleaved-edge-overgrowth technique [2], the electron density is decreased by an external gate voltage above the wire region. Eventually, the density becomes so low that impurity potentials traverse the Fermi energy, and a one–dimensional quantum island is formed between two such impurities. Since we can treat the low energy properties of one–dimensional interacting electrons in terms of Luttinger liquid theory, the role of many body effects can be investigated. In particular, the interfacing between the quantum dot and the leads is technologically important and

byproducts of the effort in understanding transport through such nanostructures may lead to operational criteria for future devices.

2 Model

We use the bosonization technique [5, 6] for interacting electrons in 1D. The quantum dot is described by a double barrier consisting of two delta-function potentials $V_i \delta(x - x_i)$ at x_i $(i = 1, 2)$ where $x_1 < x_2$. An external electric field $\mathcal{E}(x, t) = -\partial_x U(x, t)$ is assumed to induce transport. The Hamiltonian is

$$H = H_0 + H_1 + H_2. \tag{1}$$

The first term describes the interacting electrons as a Luttinger liquid [3, 4],

$$H_0 = \frac{\hbar v_F}{2} \int dx \left[\Pi^2(x) + [\partial_x \vartheta(x)]^2 \right] + \frac{1}{\pi} \int dx \int dx' \, \partial_x \vartheta(x) \, V(x - x') \, \partial_{x'} \vartheta(x') \tag{2}$$

The electrons are represented by conjugate *bosonic plasmon fields* $\Pi(x, t)$ and $\vartheta(x, t)$ which are associated with the collective charge density excitations. The system length is L and the Fermi velocity v_F. The interaction, $V(x - x')$, is a projection of a modified 3D Coulomb interaction onto the x-direction (see below). It has the Fourier transform $\hat{V}(q)$, which is the dominant quantity in the dispersion relation of the collective charge excitations

$$\omega(q) = v_F |q| \left[1 + \frac{\hat{V}(q)}{\pi \hbar v_F} \right]^{1/2}. \tag{3}$$

The dispersion relation for free electrons would be linear ($\omega(q) = v_F|q|$). The transport inducing electric field (slowly varying with respect to k_F^{-1}) couples to the long wavelength parts of the charge density $\rho(x) \approx \rho_0 + (1/\pi)^{1/2} \partial_x \vartheta(x)$. Here $\rho_0 = k_F/\pi$ is the mean electron density. This yields

$$H_2 = -e\sqrt{\frac{2}{\pi}} \int dx \, U(x, t) \partial_x \vartheta(x). \tag{4}$$

Finally, the two localized impurities define the left and right lead and the quantum dot itself between the impurities. Their contribution is

$$H_2 = \rho_0 \sum_{i=1,2} V_i \cos \left[2k_F x_i + 2\sqrt{\pi} \vartheta(x_i) \right] \tag{5}$$

Because of gates and surrounding charges in the actual experiments, screening is always present for the mutual electron interaction. We model this situation in terms of a 3D Coulomb interaction, an infinite metallic gate in distance D to the quantum wire, and parabolic confinement perpendicular to the wire. The effective interaction potential is then obtained by using the method of image charges and projecting onto the wire axis with a normalized Gaussian confinement wavefunction. This leads to the Fourier transform of the effective interaction potential [7]

$$\hat{V}(q) = V_0 \left[e^{d^2 q^2/4} \, \mathrm{E}_1 \left(\frac{d^2 q^2}{4} \right) - 2\mathrm{K}_0(2Dq) \right], \tag{6}$$

where $V_0 = e^2/4\pi\epsilon_0\epsilon$, $\varepsilon_0\epsilon$: dielectric constant, $D \gg d$: gate distance and wire diameter, $\mathrm{E}_1(z)$: exponential integral, and $\mathrm{K}_0(z)$: modified Bessel function [8].

3 Effective Action

For determining the transport properties through the system it is sufficient to know the behavior of the plasmon fields at the barrier positions x_1 and x_2. Hence, we calculate an effective action for the symmetric and antisymmetric variables for the density

$$N^\pm = \frac{1}{\sqrt{\pi}}\left[\vartheta(x_2) \pm \vartheta(x_1)\right],\tag{7}$$

which are related to the excess particle number on the island between the two impurities $(-)$ with respect to the mean value. The $+$-sign refers to the number of im–balanced particles between the left and right lead. The effective action is evaluated by use of an imaginary-time path integral method [9] and reads

$$
\begin{aligned}
S_{\text{eff}}[N^+, N^-] &= \int_0^{\hbar\beta} \mathrm{d}\tau\, H_2[N^+, N^-] - \sum_{r=\pm} N^r(\tau)\mathcal{L}^r(\tau)\\
&\quad + \frac{1}{2}\sum_{r=\pm}\int_0^{\hbar\beta}\int_0^{\hbar\beta}\mathrm{d}\tau\mathrm{d}\tau'\, N^r(\tau)K^r(\tau-\tau')N^r(\tau').
\end{aligned}\tag{8}
$$

The dissipative kernels $K^\pm(\tau)$ and the effective driving force $\mathcal{L}^\pm(\tau)$ capture the effects of the interaction through the dispersion relations (3) of the collective modes. While $\mathcal{L}^\pm(\tau)$ describes the effect on the external field and is considered elsewhere [7], $K^\pm(\tau)$ is associated with the charging energy and the spectral properties of the island. It has the Fourier transform at Matsubara frequencies $(L \to \infty)$

$$\left[K^\pm(\omega_n)\right]^{-1} = \frac{4v_{\text{F}}}{\hbar\pi^2}\int_0^\infty \mathrm{d}q\frac{1 \pm \cos[q(x_1 - x_2)]}{\omega_n^2 + \omega_\nu^2(q)}.\tag{9}$$

4 Results

At low temperatures the transport through the quantum island is dominated by charging effects. The *linear conductance* shows discrete maxima which correspond to the transfer of single electrons through the dot. The peaks occur whenever the chemical potentials of the leads and the quantum dot are aligned. Otherwise, transport is blocked (Coulomb blockade). By applying a gate voltage to the island, the situation of waved Coulomb blockade can be achieved periodically and one obtains so–called Coulomb blockade oscillations. The distance between the conductance peaks with respect to the gate voltage is then directly related to the charging energy of the dot and experimentally accessible. From equation (9) an analytic, microscopic expression for the charging energy is readily obtained in the static limit: $E_{\text{C}} = K^-(\omega_n \to 0)/2$. For free electrons, the charging energy is only due to the Pauli exclusion principle and can be evaluated analytically: $E_{\text{free}} = \pi\hbar v_{\text{F}}/2a$. Generally, the charging energy depends on the system parameters through the dispersion in equations (3) and (6). The parameters are interaction strength V_0, interaction range which is basically determined by the distance of the gate D, the length of the island a, and the wire diameter d. Fig. 1 shows the numerically evaluated charging energy for realistic experimental values [1]. We find that the charging energy increases with increasing interaction range D. For a very large D, an asymptotic value is reached. This is because in the beginning, the increasing range makes it harder for electrons to get on
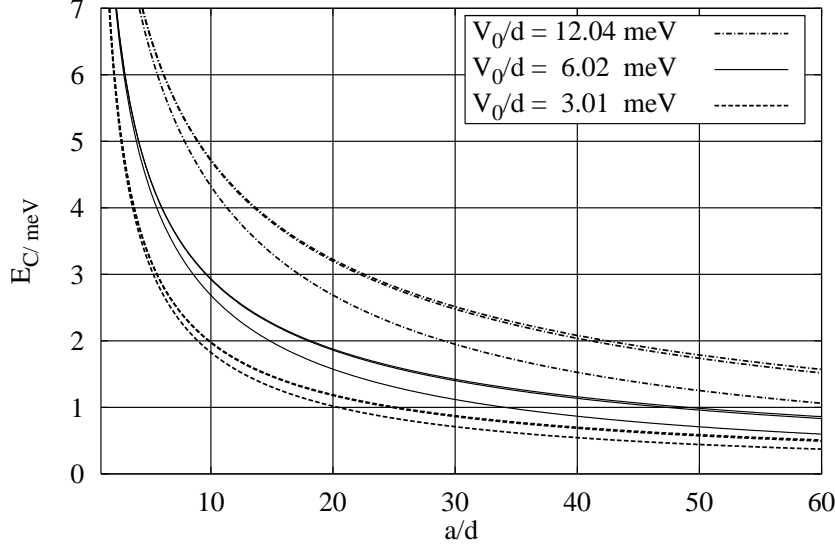
Figure 1: Charging energy E_ρ in meV as a function of a/d (Fermi energy $E_F = 3\,\text{meV}$, effective electron mass $m = 0.067m_0$), $d = 20\text{nm}$, interaction strengths $V_0/d = 12.04\,\text{meV}$ (dashed-dotted), $6.02\,\text{meV}$ (full lines,) and $3.01\,\text{meV}$ (dotted), corresponding to $\epsilon = 3, 6, 12$, $D/d = 500, 50, 5$ (top to bottom).

the island. But increasing the range even further by a large D with respect to the island length a does not change the charging energy significantly because the repulsion between the electrons *on* the island is the dominant contribution. Certainly the charging energy increases when the overall interaction strength V_0 is increased. We find consistent values for charging energy and island length for the experimental parameters of Ref. [1] within our microscopic approach.

The frequency-dependent parts of the kernels describe the dynamic effects of the external leads and of the correlated excited states in the dot. Their influence is described by spectral densities $J_\nu^\pm(\omega)$ which are related to the imaginary-time kernels via analytic continuation.

$$J(\omega) = \frac{1}{\pi\hbar} \sum_{\nu=\pm} \text{Im} K^\nu(\omega_n \to +\text{i}\omega) \,. \tag{10}$$

For our realistic long ranged interaction (6) analytic expressions for these densities are not available, but we can learn about their properties by using a "long range toy" interaction $V^\text{toy}(x) = 2V_0/(\alpha d)^2 \exp(-\alpha|x|)$ where α is a phenomenological screening parameter which determines the range of the interaction. The relatively simple form of the Fourier transform of this interaction allows for the analytical calculation of the nonlocal conductivity of a pure quantum wire [12]. The kernel (9) can also be written in terms of the conductivity. Lengthy but straightforward calculations finally yield the spectral density. This spectral density is plotted in Fig. 2 for three different α. It displays the following features due to the long range interaction: there are broadened, delta-function-like peaks which tend to become equidistantly spaced for large ω. The peaks become very narrow for large energies. This effect is enhanced when the range of the interaction is decreased.
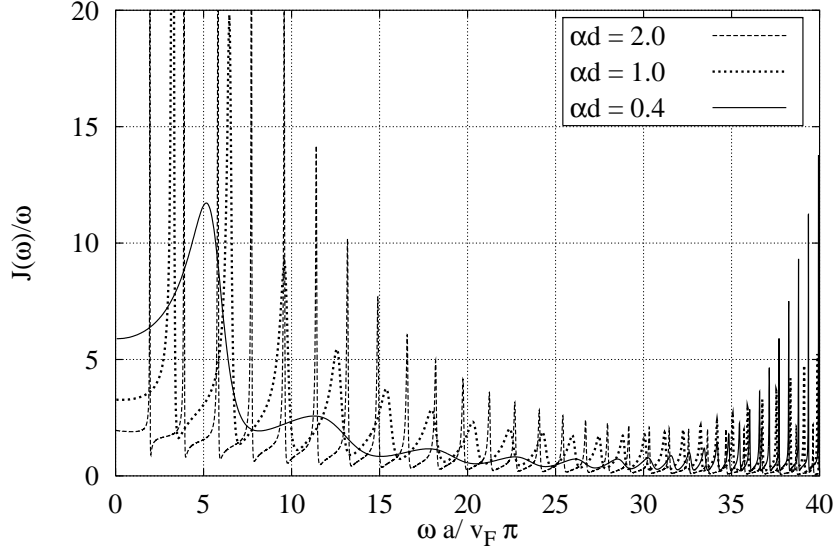
Figure 2: Spectral densities $J(\omega)/\omega$ for the interaction $V(x) = 2V_0/(\alpha d)^2 \exp(-\alpha|x|)$ as a function of normalized frequency $\omega a/v_\mathrm{F}\pi$ where $a/d = 10\pi$ and $g_0 = [1 + V_0/(\hbar\pi v_\mathrm{F})]^{-1/2} = 0.5$. The interaction range is tuned by $\alpha d = 2, 1, 0.4$ (increasing range).

Actually the limit $\alpha \to \infty$ leads to non-interacting electrons as seen in the form of V^{toy}. Further, the peaks are strongly broadened when the interaction range is increased. Again, for a large ω, independent of the value of α, the peaks become narrow, almost delta-function-like peaks, and attain an equidistant spacing which we would expect for non-interacting electrons in one dimension which are confined to a region of length a. We suggest the following interpretation: the interacting electrons are described by their collective excitations in terms of the plasmon fields. The barriers pin these plasmons and a situation similar to a standing wave occurs. The excitation energies of the system then approximately correspond to $\omega(q_m = m\pi/a)$. This explains why the maxima are shifted when the interaction range is increased. It is due to the nonlinearity of the dispersion relation for the plasmons at "smaller energies" while the dispersion becomes linear again after a certain energy ω_p [12]. On the other hand, the effective Hamiltonian is equivalent to one for a quantum Brownian particle (corresponding to the coordinates $N^\pm$) in a dissipative environment and external potential. In this context the spectral density describes the possible "channels" for energy dissipation between the environment and the Brownian particle in a potential. One finds in the zero-range case that the peak positions correspond to (single) particle states in the dot. This analogy leads us to interpreting the peaks as states of the quantum dot which may contribute to transport through the dot. Because the interaction couples the dot with the leads, the "levels" of the quantum dot are broadened. The leads contribute mainly to the spectral density through a quasi Ohmic background. In the case of free electrons, the spectral density can be separated into a sum of delta function peaks describing the states of the dot and an Ohmic part ($\propto \omega$) corresponding to the leads. This separation also works if one takes a zero-range interaction. Basically this tells us that a zero-range interaction creates an isolated

quantum dot coupled to leads. Taking into account a long-range interaction, accounts for the correlation effects better, and the corresponding spectral density describes the overall spectral properties of the entire system including the left lead, the dot and the right lead. To sum up, first the interaction shifts the energy levels of the dot, and second the levels are broadened due to the coupling to the leads.

Though we are unable to calculate the complete spectral densities for our realistic interaction (6) we can obtain the limits for $\omega \to 0$,

$$J(\omega \to 0) = \frac{\omega}{2g} \left[1 + g^4 \left(\frac{2aE_{\mathrm{C}}}{\pi \hbar v_{\mathrm{F}}} \right)^2 \right], \tag{11}$$

where $g^{-2} = 1 + \hat{V}(q \to 0)/\pi \hbar v_{\mathrm{F}}$ and E_{C} is the charging energy. This limit describes the dissipative influence of the low-frequency charge excitations in the external leads, $x < x_1$ and $x > x_2$. It holds also for finite frequencies. However, these must be smaller than the frequency scale corresponding to the range of the interaction, and smaller than the characteristic excitation energy of the correlated electrons in the dot. One can show that the intrinsic width $\Gamma(T)$ of the conductance peaks of the Coulomb oscillations exhibit a nonanalytic power-law due to the interaction [10, 11]. The exponent is directly related to the limit in eq. (11). Defining $1/g_{\mathrm{eff}} := J(\omega \to 0)/\omega$ we write for the temperature dependence $\Gamma(T) \propto T^{1/g_{\mathrm{eff}} - 1}$ [7]. In contrast to a treatment with zero-range interaction, the exponent depends in a nontrivial way on the geometry of the system and the parameters of the interaction reflected by the charging energy $E_{\mathrm{C}}(a, D, V_0)$ in eq. (11). In the zero-range case g_{eff} becomes simply equal to g and the coupling of the dot seems to be disguised – only the properties of the leads are manifest in terms of g. Thus the long range nature of the interaction should be manifest in the shape of the Coulomb peaks in experiments.

5   Conclusion

We derived an effective action for a double barrier in a quantum wire taking account the interactions in terms of Luttinger liquid theory. We discussed the effect of a realistic, long-range interaction on the charging energy which relates to the distances between Coulomb blockade peaks. The spectral properties of the system are examined by resorting to a simpler "toy interaction" which shows the basic features of long range interaction. The spectral density of the system is compared to the case of the usual zero range Luttinger liquid interaction. Finally, the effect of the interaction on the shape of the linear conductance Coulomb peaks is mentioned.

This contribution only highlights the role of the charge degree of freedom. One can also include effects due to the electron spin [7]. In the bosonized picture, the degrees of freedom are decoupled and develop charge and spin collective excitations respectively. In addition to the results above spin addition energies and spin excited states appear. Also, the power law for intrinsic width of the Coulomb peaks acquires a spin dependence.

References

[1] O. M. Auslaender, A. Yacoby, R. de Picciotto, K. W. Baldwin, L. N. Pfeiffer, and K. W. West, Phys. Rev. Lett **84**, 1764 (2000).

[2] A. Yacoby, H. L. Störmer, K. W. Baldwin, L. N. Pfeiffer, and K. W. West, Solid State Comm. **101**, 77 (1997).

[3] S. Tomonaga, Prog. Theor. Phys. **5**, 544 (1950).

[4] J. M. Luttinger, J. Math. Phys. **4**, 1154 (1963).

[5] F.D.M. Haldane, J. Phys. C **14**, 2585 (1981).

[6] J. Voit, Rep. Prog. Phys. **57**, 977 (1995).

[7] T. Kleimann, M. Sassetti, B. Kramer, and A. Yacoby, Phys. Rev. B **62**, 8144 (2000).

[8] M. Abramowitz, and I. A Stegun, *Handbook of Mathematical Functions*, (Dover Publ., New York 1965).

[9] M. Sassetti, and B. Kramer, Phys. Rev. B **54**, R5203 (1996).

[10] A. Furusaki, and N. Nagaosa, Phys. Rev. B **47**, 3827 (1993).

[11] A. Braggio, M. Grifoni, M. Sassetti, and F. Napoli, Europhys. Lett., **50**, 236 (2000).

[12] G. Cuniberti, M. Sassetti, and B. Kramer, Phys. Rev. B **57**, 1515 (1998).